Received: 21 September 2021 | Accepted: 23 September 2021

DOI: 10.1111/mmi.14816

MICROREVIEW

WILEY

Microfabrication and its use in investigating fungal biology

Tina Bedekovic | Alexandra C. Brand

Medical Research Council Centre for Medical Mycology, University of Exeter, Exeter, UK

Correspondence
Alexandra C. Brand, Medical Research Council Centre for Medical Mycology, University of Exeter, Geoffrey Pope Building, Stocker Road, Exeter EX4 4QD, UK.
Email: a.brand@exeter.ac.uk

Funding information
This work was funded in whole, or in part, by the Wellcome Trust (grant no. 206412/A/17/Z). For the purpose of open access, the author has applied a CC BY public copyright license to any Author Accepted Manuscript version arising from this submission. The work was also supported by a Royal Society URF (UF080611), MRC NIRG (G0900211/90671), and the MRC Centre for Medical Mycology at the University of Exeter (MR/N006364/2)

Abstract

Advances in microfabrication technology, and its increasing accessibility, allow us to explore fungal biology as never before. By coupling molecular genetics with fluorescence live-cell imaging in custom-designed chambers, we can now probe single yeast cell responses to changing conditions over a lifetime, characterise population heterogeneity and investigate its underlying causes. By growing filamentous fungi in complex physical environments, we can identify cross-species commonalities, reveal species-specific growth responses and examine physiological differences relevant to diverse fungal lifestyles. As affordability and expertise broadens, microfluidic platforms will become a standard technique for examining the role of fungi in cross-kingdom interactions, ranging from rhizosphere to microbiome to interconnected human organ systems. This review brings together the perspectives already gained from studying fungal biology in microfabricated systems and outlines their potential in understanding the role of fungi in the environment, health and disease.

KEYWORDS
hyphal growth responses, population heterogeneity, yeast replicative aging

1 | INTRODUCTION

For nearly 400 years, microscopes have enabled us to explore and describe the diversity of fungi and to observe the effect of experimental manipulations of the cell population. In the last few decades, three new technologies have transformed our application of microscopes in understanding fungal biology and real-time processes in individual cells. First, computer programmable light microscopes enabled real-time imaging of living cells over periods of hours and days to follow temporal processes; second, molecular genetics enabled us to alter gene expression and track fluorescently tagged proteins and reporters inside cells to understand mechanisms. Third, transferred from the semi-conductor industry, microfabrication methods now allow us to manipulate the physical and chemical environment of individual living cells in real-time in situ on the microscope. This "lab-on-a-chip" technology is now extending into complex multi-cell and compartmentalized environments in "organ-on-a-chip" applications (Last et al., 2021). The contribution of microfabricated surfaces to our understanding of the biology and interactions of fungal cells is just beginning. This review will discuss the contribution that microfabrication has made to the study of biologic processes of yeast, the exploratory growth of hyphae, and how the viscoelastic properties of soft polymer "chips" have been exploited to quantify fungal force and its impact on fungal morphology.

2 | BASIC FORMATS OF MICROFABRICATED SURFACES USED IN FUNGAL RESEARCH

Microfabrication is the process through which topographies are generated on an inert material at the micrometer scale (or smaller) in the planar (x, y), and vertical (z) dimensions, where bespoke designs are generated to address specific biological questions. Key to

the technology is the ability to engrave, etch, and now write, micropatterns onto an inert surface. Over the last 4 decades, there have essentially been three developmental steps in the use of these surfaces. In early systems, the design of interest was patterned directly onto a surface as a "positive" on which cells were grown. Although this is still used for some applications, it was superseded by designs patterned as a "negative" from which multiple positives could be copied, or cast, using a soft polymer. Finally, as resolution improved, systems could be perfused with liquid or pressurized with gas, unlocking the door to longer-term experiments and the ability to create, image, and manipulate the micro-environment in situ.

2.1 | Unenclosed microfabricated surfaces

Early use of microfabricated surfaces involved engraving or etching nanopatterned topographies directly onto an inert, resilient surface, such as quartz (Figure 1a). Fungal spores or yeast cells were inoculated at low density onto the surfaces and, depending on the species, were submerged if necessary in a suitable growth medium. For example, hyphae germinating from spores, or from yeast cells of the pleomorphic fungus, *Candida albicans*, were imaged after growth across the micropatterned surface by light or Scanning Electron Microscopy (*SEM*) to characterize thigmotropic (contact-sensing) responses. The cost of the substrate materials used as "positive" topographies was relatively high so they were cost-effective only if they could be reused. This meant that coverslips used for microscopy could not be sealed with a substance that could not be completely removed. Adhered fungal cells also had to be removed, usually by soaking the material in concentrated acid, which was easily washed off inert substrates. The major limitation of an unenclosed system is that imaging occurs at the endpoint, thus limiting its use to investigating whole-cell responses, morphology changes, and overall growth strategies. Although this approach has been superseded by the ability to take multiple castings from a negative master template using a cheap and inert polymer, such as polydimethylsiloxane (PDMS), the advent of 3D printers of increasingly high resolution means these positive surfaces can be generated more cheaply, which is advantageous if the research question requires freedom of growth in the vertical dimension.

2.2 | Static chambers

The development of photolithography on silicon wafers both reduced the cost of microfabricated materials and increased their range of applications. A static chamber consists of a PDMS micropatterned chip, cast from a negative silicon wafer master, onto which cells are inoculated at low density along with a growth medium (Figure 1b) or introduced at one end on a mycelial plug. A coverslip is supported by the raised surface features and sealed around its edge with a nontoxic sealant such as melted valapa (a 1:1:1 ratio of Vaseline, lanolin, and paraffin wax). The resulting chamber both immobilizes the cells and retains the growth medium. Although they are basic, static chambers provide a simple and effective method for live-cell imaging at the whole cell and the molecular levels using Differential Interference Contrast (DIC) coupled with fluorescence microscopy. As the system is sealed, it can be viewed on upright or inverted microscopes until the medium is spent (~7 hr for *C. albicans*). An advantage of this system over unenclosed surfaces is that hyphae are constrained by the coverslip to grow only in the *x* and *y* dimensions and do not become out of focus through undulation in *z*. With the use of a motorized stage, multipoint-visiting microscopy can quickly capture dozens of images across a relatively wide area, both improving the opportunity to identify rare events in real-time yet sampling hundreds of cells for robust statistical analysis.

The primary costs in this system derive from producing the silicon wafer featuring multiple repeats of a negative version of the topography of interest from which PDMS positives are cast and excised. Some labs generate a positive master wafer from which several negatives are cast in epoxy resin, which requires the use of a release agent. The availability of multiple epoxy negatives speeds up chip generation and minimizes the inevitable damage to the relatively fragile silicon master. As with unenclosed systems, the design of surface micropatterning is dependent on the research question and the dimensions of the fungus, so require careful consideration. Some general-purpose designs for the masks used to generate silicon wafer patterning can be acquired as computer-aided design (CAD) software files from published authors but most applications require bespoke patterning. Static microfabricated chambers have proved valuable through their relative simplicity and accessibility and have facilitated the study of a breadth of topics including fungal mechanics, intracellular dynamics, and fungal growth responses within the physical environment (Bedekovic et al., 2020; Brand et al., 2008; Minc et al., 2009; Puerner et al., 2020; Thomson et al., 2015).

2.3 | Microfluidic systems—Lab-on-a-chip

By incorporating input–output perfusion channels and complex internal features into the PDMS chip design, experiments that alter the chemical environment of the fungus by switching input channels or generating gradients can be carried out (Figure 1c). Importantly, only very small volumes of often costly compounds such as inhibitors, stress factors, pheromones, drugs, antibodies, or cell stains are required. Perfusion involves the insertion of blunt biopsy needles carrying silicone tubing into the entry and exit ports designed into the chip, with the use of gravity-fed, peristalsis pump, or syringe pump-driven delivery. Pretreatment of both the coverslip and the patterned PDMS surface in a plasma cleaner ensures strong bonding of the surfaces to avoid leakage and maintain isolation between the flow channels. For ease of use, perfused systems generally require the use of an inverted microscope. Multipoint visiting microscopy increases efficiency as parallel channels containing different organisms, mutants, or environments can be imaged in a single experiment. The ability to perfuse for long periods and image cells while manipulating the environment in situ lead to the term 'lab-on-a-chip'

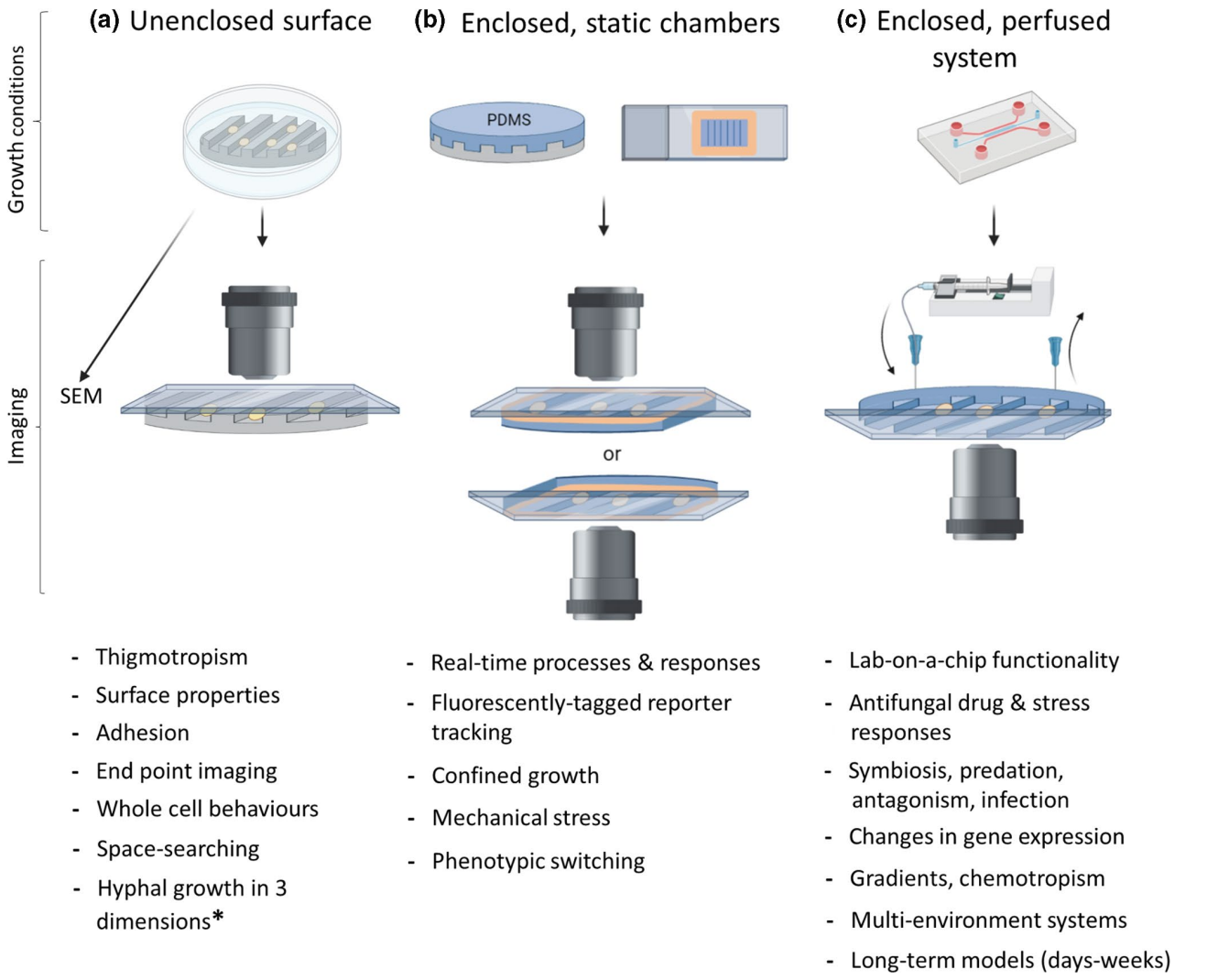

FIGURE 1 Basic microfabricated formats used in fungal research. The use of microfabricated surfaces in fungal research has progressed through three formats. Each format from left to right confers the additional functionality listed compared with its predecessor. *The exception is "hyphal growth in three dimensions," where the unenclosed system allows unconstrained growth in the *z* plane. (a) Unenclosed surface: cells are inoculated at low density onto a reusable micropatterned substrate such as quartz. After culturing, a fixative and/or a stain can be applied, if required, before a coverslip is placed on top and the substrate imaged on an upright microscope. Alternatively, the substrate can be gold-sputtered and imaged using a Scanning Electron Microscope (SEM). (b) Enclosed static chambers: PDMS-positive replicas are cast from a negative pattern etched onto a silicon wafer. Cells are inoculated at low density in a liquid medium or introduced as a mycelial plug. A coverslip is applied and sealed around the edges to retain a liquid growth medium and moisture. Live-cell imaging can be undertaken on an inverted or an upright microscope. (c) Enclosed perfused system: microfluidics functionality using a PDMS-positive replica cast from a negative pattern with input/output perfusion channels. Designs can range from simple viewing chambers to complex arrays of compartments containing niche environments and cell types. Figure generated in BioRender

and provided a step change in the types of experiments that can be undertaken. These systems can incorporate mechanisms to generate concentration gradients through complex mixing or parallel flow diffusion channels within the chip in order to fine-tune exposure to drugs and other reagents (Lee et al., 2020; Saka et al., 2017; Witkowski et al., 2018). Bespoke designs have also been used to study multispecies interactions, including biocontrol approaches and metabolite exchange in fungus–bacteria symbiosis (Gimeno et al., 2021; Uehling et al., 2019). However, in this review, we focus on how microfabrication has been used to enhance our understanding of yeast and hyphal growth.

3 | USE OF MICROFABRICATED SYSTEMS TO STUDY REPLICATIVE AGING AND GENE EXPRESSION IN YEAST

Replicative cell aging (the numbers of daughter cells produced prior to cell cycle arrest) and its causes have long been studied in the model yeasts, *Saccharomyces cerevisiae* and *Schizosaccharomyces pombe*, using methods such as cell sorting and micromanipulation (Barker & Walmsley, 1999). Microfabricated formats, in the form of perfused microfluidic systems, have proved ideal for capturing and imaging populations of mother cells in real time at the level of individual cells.

Using different trapping systems that accommodate asymmetrical budding in *S. cerevisiae* and symmetrical fission in *S. pombe*, daughter cells can be removed from the system to avoid overgrowth.

For *S. cerevisiae*, two types of trapping systems have been used that exploit the size difference to retain larger mother cells while smaller daughter cells are washed away by perfused laminar flow (Chen et al., 2017; Crane et al., 2014; Lee et al., 2020; Ryley & Pereira-Smith, 2006). Horizontal traps capture and retain cells through flow, while the ceilings of vertical traps are raised by increasing the internal pressure (of liquid or air) during cell inflow, then lowered by decreasing the pressure to trap the cells, which can then be imaged for 5–7 days. The replicative lifespan of *S. cerevisiae* was quantified as ~25 cell divisions (similar to *C. albicans*), which slowed with age. However, the microfluidics platform revealed that there was considerable population heterogeneity in cell cycle duration and cell death in aging yeast cells that was driven by multiple causes (Crane et al., 2014; Fu et al., 2008; Lee et al., 2012). Dietary restriction has long been associated with prolonged lifespan but microfluidics approaches produced inconclusive results when used to examine this in *S. cerevisiae* (Huberts et al., 2014; Jo et al., 2015). Thus, the challenge is to understand the impact of device design and experimental conditions on the biology of the organism of interest. To ask whether the geometry of the cell trap and the age-dependent size/morphology of the mother cell causes compression stress during media flow and budding, Crane et al. monitored stress in their ALCATRAS system (A Long-term Culturing And TRApping System) by observing translocation of the general cell-stress marker, Msn2, into the nucleus (Crane et al., 2014). They found this occurred only sporadically and at the same rate as in nonconstrained cells. In contrast, Msn2 nuclear translocation was observed during periods of glucose limitation, although the percentage of cells responding to nutrient stress reduced with each treatment. To ask whether the reduced response was attributable to the onset of senescence, stress was imposed in populations of young and old cells and showed that the reduction resulted from cell history, or memory, and not due to cell aging. The ability to manipulate the cell environment within microfluidic systems, therefore, provides a method to study long-term effects on individual cells.

For *S. pombe*, replicative aging studies have used a microfluidic architecture known as the "Mother Machine", originally designed for studying the rod-like bacterium, *Escherichia coli* (Nakaoka & Wakamoto, 2017; Wang et al., 2010). Cells were entrapped within a tube that was closed off at one end so the original mother cell was easily identifiable as the cell at the closed end of the tube. New daughter cells eventually protruded from the open end and were washed away. In contrast to budding yeast, replicative aging appeared to be absent in *S. pombe*, as up to 80 generations were monitored in seven different growth conditions. Furthermore, protein aggregation, which has long been considered as a marker of cell aging, did not affect lifespan. Microfluidic systems have therefore challenged findings concerning two factors thought to influence cell aging—nutrient limitation and protein aggregation—but also offer the means through which they can be further investigated.

Different types of stress can be applied within microfabricated systems and, coupled with the expression of GFP reporter proteins, this approach has offered novel perspectives in yeast cell biology. Using cells expressing the heat shock reporter, HSP104-GFP, Ryley and Pereira-Smith found that exposure to 42°C for 2 hr induced wide population variation, not only in levels of HSP104-GFP expression (range = 2.6–9.6-fold) but in the time taken to reach peak expression (3–5 hr post-treatment), demonstrating significant population heterogeneity (Ryley & Pereira-Smith, 2006). Additionally, a study of yeast signaling cross-talk found that cells exposed to 0.1–0.15 M NaCl formed two distinct subpopulations—those that upregulated the osmo sensor, Stl1, and those that did not, a finding that may have been missed using other approaches (Lee et al., 2020). Single-cell microscopy has additionally identified treatment-dependent localization of the GFP-tagged MAPKKK, Pkc1. In cells exposed to H_2O_2, Pkc1 formed cytoplasmic foci, but mechanical stress localized it to the plasma membrane. This observation provided further insights into specific stress response mechanisms and how, through differential spatial positioning, Pkc1 operates in diverse signaling pathways (Lee et al., 2020). Together, these findings highlight the diversity of cell responses within a population that can be identified and dissected in microfabricated systems.

4 | USE OF MICROFABRICATED TOPOGRAPHIES TO STUDY HYPHAL GROWTH RESPONSES

Many more filamentous fungi than yeast species have been studied using microfabricated systems. Most applications have used various designs of channels, mazes, or obstacles to test the hyphal directional growth responses and exploration strategies of environmental or pathogenic fungi that cannot be imaged within opaque soil or host tissue. One of the earliest applications of microfabrication in fungal research was the study of the thigmotropic (contact-guided) growth of phytopathogens. Spores were germinated on micropatterned topographies in unenclosed systems and hyphae then viewed by light microscope or *SEM*. These studies revealed that the hyphal tips of plant pathogens, such as *Uromyces appendiculatus* (bean rust fungus), grow with an asymmetrical "nose-down" morphology on surfaces (Figure 2a; Hoch et al., 1993). In a comparison of 27 species of rust fungi grown on surfaces that mimicked the dimensions of host leaf ridges and stomatal guard cells, nine, including *Uromyces* spp. and *Puccinia* spp., used thigmotropism to navigate across surface depressions in order to locate penetration points. In addition, ridges with an optimal height of 0.4–0.8 μm induced the formation of appressoria (Allen et al., 1991; Kwon & Hoch, 1991; Read et al., 1997). These surfaces thereby demonstrated the importance of mechanical cues and their specificity in locating a suitable fungal penetration point, independent of host surface chemistry. Later studies of the human pathogen, *C. albicans*, growing on an unenclosed surface incorporating ridges with heights less than half the hyphal diameter, showed that the

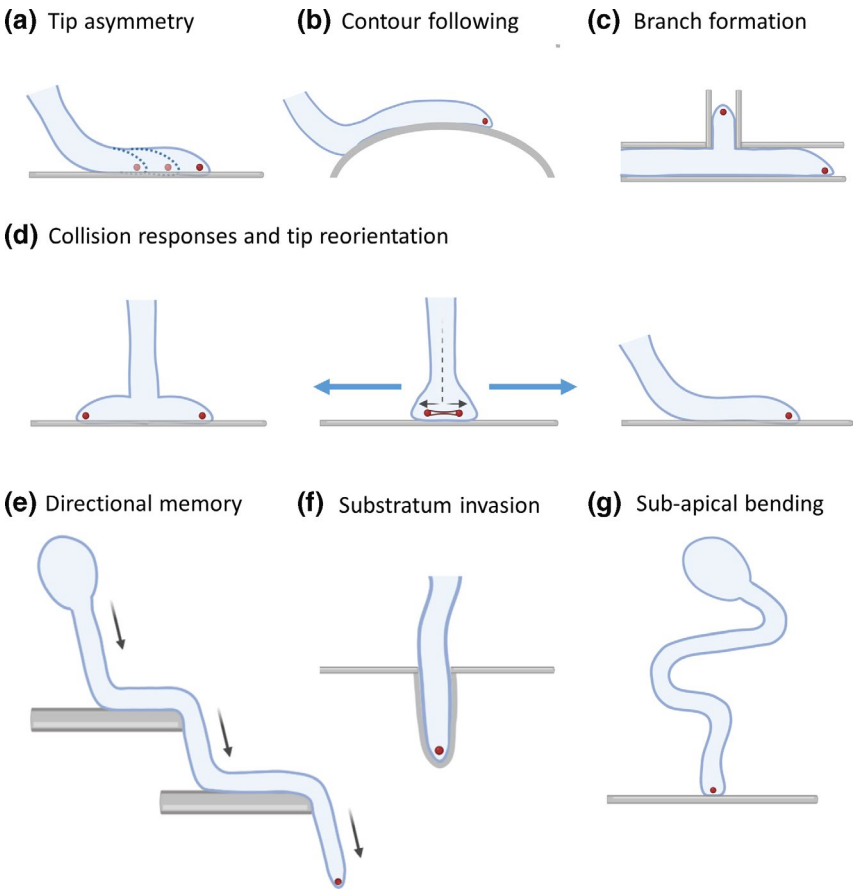

FIGURE 2 Hyphal growth responses to microfabricated topographies. Commonly observed hyphal responses to physical features. (a) Hyphal tips adopt a "nose-down" morphology with asymmetrical distribution of the Spk toward the point of tip contact with an obstacle. (b) Tip asymmetry directs hyphal growth along obstacle contours. (c) True filamentous fungi (e.g., *Neurospora crassa*) generate branches that extend into side channels. (d) Orthogonal tip collisions with an obstacle lead to apical membrane distension and distortion of the Spk (center). In *N. crassa* (left), the SPK disintegrates before establishing two new polarity axes in apical tip splitting. In *Candida albicans* (right), the Spk oscillates and deforms but retains integrity before moving into the reoriented apical growth zone. (e) Directional memory: growing hyphae are deflected around small obstacles but maintain their initial growth trajectory. (f) Substratum invasion: hyphal tip collisions with a substrate of low Young's modulus (stiffness) lead to penetration of the substrate, but only when the hyphal adhesive force (or physical immobilization) is sufficient to counter the applied tip force. (g) Subapical bending or buckling: When the hyphal tip force exceeds the adhesive force, cell wall elasticity allows hyphae to bend or buckle to accommodate the protrusive force of continued tip growth. For references, see text. Figure generated in BioRender

nose-down morphology of hyphal tips is essential for their ability to detect and respond to relatively small topographical features (Figure 2a), as these were ignored by hyphae that did not adopt this morphology due to the deletion of the polarity GTPase, Rsr1 (Brand et al., 2008).

More recently, studies using enclosed systems have examined hyphal growth rate, branching patterns, and navigation strategies within laterally confined channels, complex maze-like structures, and 2D spaces. Although these studies reveal that environment differentially impacts growth rate and branching in a species-specific manner, they also point to several commonalities in fungal morphology and exploratory behavior. All filamentous fungi tested grow more slowly in microfabricated chips than on agar and this is exacerbated by close confinement in channels: for example, the growth rate of the ascomycete, *Neurospora crassa*, was 15.6-fold slower in confined channels compared with growth on agar (Baranger et al., 2020; Held et al., 2011). High-resolution imaging of this fast-growing fungus was nevertheless aided by a lateral spiral channel chip design that retained the whole hypha within the field of view (Lee et al., 2016). Perfusion and channel trajectory, however, exert different effects on fungal species. In a study of seven Basidiomycetous litter-decomposing fungi, an "Obstacle Chip" containing air-filled channels was inoculated by placing mycelial plugs at the entrance (Aleklett et al., 2021). In the absence of a liquid medium, hyphal growth was sustained solely by transport of nutrients from the plug for periods of up to ~60 days, although there was large species-specific variation in the growth rate and distance attained. In channels containing angular turns of ≥90°, most fungi grew more slowly than in straight channels, but two species, *Mycetinus scorodonius* and *Gymnopus confluens*, grew further in channels containing sharp turns, although the biology underlying this has yet to be elucidated. In a comparison of hyphal

elongation in perfused versus nonperfused channels, *Talaromyces helicus* was found to be perfusion-insensitive, whereas *N. crassa* increased its elongation rate from 190 to 300 μmh^{-1} in perfused channels (Baranger et al., 2020). Neither perfusion flow rate nor the direction of flow appears to affect the rate of fungal growth or the direction of spore germination (in 0.8 μlh^{-1}). Together with the finding that perfusion of yeast does not trigger stress signaling, there is little evidence that fungi are highly sensitive to shear stress, although this remains to be explored (Baranger et al., 2020; Crane et al., 2014; Fukuda et al., 2021).

A panel of seven fungi was used to examine whether the ratio of channel width to hyphal diameter affected elongation and was not a straightforward predictor of whether a hypha could successfully grow through a constriction (Fukuda et al., 2021). Instead, it was the fungal growth rate that played a predominant role. Slow-growing fungi—*Aspergillus nidulans*, *A. oryzae*, and *Fusarium oxysporum*—successfully grew through a 1 μm channel, whereas fast-growing *Rhizopus oryzae*, *Coprinus cinerea*, and *N. crassa* were unable to maintain polarized growth. On further investigation using *N. crassa* in which Chs1-GFP was expressed as a marker of the Spitzenkörper (Spk), the large hyphal tip volume of secretory vesicles generated during fast growth was redistributed subapically, along with cotransported polarity effectors and exocyst components. However, when turgor pressure, and hence growth rate, were reduced by treatment with 0.6 M KCl, *N. crassa* hyphae were able to maintain polarity and pass through the channel. Therefore, polarized growth is abolished when there is an overabundance of apical polarity components relative to the width of the constriction (Fukuda et al., 2021). Orthogonal collisions of the hyphal tip with an obstacle are another cause of disorganization of the polarity machinery. In microfabricated systems containing obstacles, collisions induced bulging of the apical plasma membrane in both *N. crassa* and *C. albicans* but led to contrasting responses that reflect the different physiology of these two ascomycetes (Figure 2d) (Held et al., 2011, 2019; Thomson et al., 2015). In multinucleate *N. crassa*, apical collisions led to disintegration of the Spk and the microtubular vesicle delivery system, before they reformed as two smaller structures, one in each pocket of the distended membrane. This initiated apical tip-splitting and the formation of two new hyphae into which nuclei were distributed. In the mononuclear fungus, *C. albicans*, where vesicle delivery is actin-based, tip collision caused the Spk (visualized using Mlc1-GFP) to stretch and oscillate across the deformed tip, but it did not disintegrate or partition. A single new growth site was established within the larger of the two membrane distensions and, as the hypha reoriented its growth along the contour, the Spk regained its normal morphology and localization. The observation that membrane expansion preceded reestablishment of normal Spk morphology and position was consistent with previous observations that a tracked Spk trailed changes in the hyphal growth trajectory. This is contrary to the idea that Spk position determines the direction of hyphal growth but this question remains to be definitively addressed (Riquelme et al., 1998; Thomson et al., 2015).

4.1 | Differential branching patterns

During growth in confined channels, branching was suppressed in filamentous fungi but resumed either when hyphae emerged from the end of the channel, or a side channel was encountered (Figure 2c) (Aleklett et al., 2021; Baranger et al., 2020; Fukuda et al., 2021; Hanson et al., 2006; Held et al., 2011). This was observed in both air-filled and nutrient-filled channels, suggesting that constriction is sensed by a signal such as contact or the build-up of a secreted factor/waste product, to negatively regulate branching. Alternatively, branching may be induced, perhaps by the increased availability of oxygen when an opening is encountered (even though PDMS is O_2 [and CO_2] permeable). Whatever the signal, it not only induces branch formation but also determines branch position so that it aligns with the side channel. Side channel sensing led to a nine-fold reduction in branching distance during growth in confined mazes compared with growth in lateral spaces or on agar, a strategy that allowed successful hyphal navigation through complex environments (Held et al., 2011). The ability to position new branches in relation to environmental cues appears to be absent in *C. albicans* as branch formation in wild-type cells occurs only adjacent to septa, whether growing as hyphae or yeast, perhaps reflecting the differing lifestyle requirements of foraging fungi compared with a human commensal.

4.2 | Hyphal tip asymmetry and directional growth responses

The early work describing hyphal tip asymmetry during growth on ridged surfaces has been advanced using enclosed systems, molecular approaches, and live-cell fluorescence microscopy. Chips designs that included obstacles revealed that contact-induced tip asymmetry has been underappreciated because microscope objectives image from a position directly above or below hyphae growing on a surface. Viewed in this way, the position of the Spk within the apex of hypha growth appears to be central. However, deconvolution of *Z*-stack images of surface-growing hyphae analyzed with rotational 3D image analysis software showed that the Spk is only central in *x* and *y* and is skewed toward the substrate in *z* (Figure 2a) (Thomson et al., 2015). Such asymmetry becomes apparent on tip contact with obstacles as the hyphal response to contact is effectively viewed from the side on (Aleklett et al., 2021; Held et al., 2019; Thomson et al., 2015). In *C. albicans*, tip asymmetry was abolished on the deletion of the polarity GTPase, Rsr1, which positions Cdc42-mediated actin cable assembly for vesicle delivery, although how contact is signaled to Rsr1 at the internal plasma membrane is not known. Contact induced not only a morphological change in the hyphal tip but skewed all the major components of the polarized growth machinery—Spk, polarisome, exocyst, and cell end markers—toward the point of contact, shown by imaging GFP-tagged reporter proteins. Tip asymmetry in *C. albicans* and *N. crassa* is important for a number of shared growth responses, including contour-following and "directional memory," in which an initial hyphal growth trajectory is maintained despite

forced navigation around a series of obstacles (Figure 2b,e). The mechanism underlying directional memory is not clear. It was abolished in *C. albicans* by the deletion of Rsr1 and, in *N. crassa*, by the deletion of ro-1, the dynein heavy chain involved in vesicle transport on microtubules (Held et al., 2011; Riquelme et al., 2000; Thomson et al., 2015). The ability of the Spk to move erratically within the tips of these mutants suggests that directional memory depends on the containment of the vesicle delivery system within a defined zone at the hyphal apex.

5 | APPLICATION OF PDMS MECHANICS IN THE STUDY OF FUNGAL FORCE

The forces generated during cell growth are exploited by fungal pathogens for the active penetration of host tissue. The tuneable viscoelastic properties of PDMS chips have proved useful in quantifying protrusive fungal force and demonstrating how substrate mechanics impact fungal growth and morphology. An important prerequisite to such studies is the need to immobilize the fungal cell, either through physical constraint or by achieving a threshold level of substrate adhesion sufficient to counter protrusive force during growth. During tip collisions with an obstacle, nonadhered hyphae maintain their tip morphology and original contact angle, either sliding along the obstacle during elongation or undergoing subapical hyphal bending (Aleklett et al., 2021; Hanson et al., 2006; Thomson et al., 2015). In contrast, direct tip collision of an adhered/immobilized hypha with an obstacle leads to apical deformation or bulging. Bulging is transient but is the point at which the applied tip force is maximal, prior to the establishment of a new growth direction. Microfabricated PDMS has been employed in two approaches to quantify this force in *C. albicans*, which invades multiple human tissue types and can even penetrate the soft silicone used in medical devices such as voice prostheses (Leonhard et al., 2013). The first approach was to generate a standard curve of applied force versus indentation distance in PDMS (with 1:10 ratio of curing agent to polymer) using atomic force microscopy incorporating a cantilevered glass bead that mimicked the dimensions of a hyphal tip (Thomson et al., 2015). The curve was used to calculate the applied force of ~8.7 μN from the indentation distance generated by hyphal tips colliding with a PDMS obstacle prior to tip reorientation. A second approach trapped yeast cells within microwells arrayed in PDMS samples of increasing stiffness (reviewed by Männik et al., 2021; Puerner et al., 2020). Once germinated, hyphae could penetrate PDMS with a Young's modulus (the relationship between applied force and substrate deformation per unit area, or stiffness) of up to 200 kPa and ~5% of hyphae could grow in even higher moduli (Figure 2f). This value is well beyond the stiffness of most body tissues, which primarily fall within the range of 0.1–35 kPa (Liu et al., 2015). The point at which resistive force equaled adhesive force was determined as 20 kPa, that is, the Young's modulus of PDMS at which the rate of growth on the surface (0.26 μm/min—approximately 20% slower than in a liquid medium) equaled that seen during embedded growth. Using a metal probe and then scaling to the size of a hypha, the breakthrough force into PDMS (1:10) was ~17 μN, approximately double that seen previously prior to tip reorientation. However, the maximum force achieved by embedded hyphae was nearly double that at 31 μN, with a stalling force of ~35 μN. Taken together, the values determined for tip force relative to Young's modulus of human tissues explain the ability of *C. albicans* to actively penetrate multiple tissue types during systemic infection.

A different microfabrication approach was used to determine tip force in *N. crassa*. Hyphae were grown in confined channels at the end of which they were confronted with a PDMS (1:10) force-sensing pillar that had to be deflected for growth to continue (Sun et al., 2018). The deflection distance of the top of the pillar was imaged and related to the precalibrated force required to generate such displacement. The maximum force for *N. crassa* was determined as 11 μN and was independent of the growth rate or the hyphal diameter. However, this was derived based on the assumption that tip contact with the pillar was made at a point equating to half the diameter of the hypha. As noted above, hyphae have a strong tendency to adopt an asymmetric tip morphology when growing on a surface so the point of contact may have differed from the assumed value. However, even if this was a factor, this low value for *N. crassa* tip force compared with *C. albicans* is consistent with a previously determined value of 3.2 μN, acquired using a strain gauge (Money et al., 2004; Sun et al., 2003). Interestingly, no instances of hyphal tip-splitting were reported in the force-sensing pillar system, where hyphal pressure displaced the obstacle, yet it occurred readily in closed PDMS geometries (Held et al., 2019). Apical splitting in *N. crassa* is therefore not signaled by an exquisite sense of touch but instead appears to result from catastrophic mechanical disruption of the polarity machinery during instances of orthogonal collision.

The growth of cells in PDMS microwells has also been used to examine the growing force generated by the fission yeast, *S. pombe* (Minc et al., 2009). In this system, bidirectionally elongating yeast cells deformed the walls of microwells, allowing a stall force of 11 μN to be determined, approximately threefold lower than *C. albicans* hyphae (Puerner et al., 2020). However, both fungi exhibited cell buckling prior to stalling that was reversed on escape or break-out from the polymer, when cells sprung back into shape. Similarly, the bulging hyphal tips of *C. albicans* and *N. crassa* instantly regained their shape when pressure was relieved by the establishment of new growth axes (Held et al., 2019; Thomson et al., 2015). The cell wall, therefore, retains its integrity under severe backward pressure from the tip and passively depends on elasticity when approaching the limit of applied tip force rather than actively undergoing significant subapical strengthening or restructuring (Figure 2g).

Microfabrication using PDMS as a substrate has proved a useful tool with which to quantify fungal force in a defined and controlled environment. However, the ability of fungi to apply force depends on the availability and uptake of solutes and water for the generation of internal turgor pressure. Further, the translation of turgor pressure into tip force depends on the regulation of cell wall plasticity (Lew, 2011; Money & Harold, 1992). Mycelial fungi can transport

water and solutes through cytoplasmic flow to maintain apical turgor pressure, while *C. albicans* can only access resources within and surrounding the apical compartment. Therefore, the biology of the fungus and the nature of its normal habitat need to be considered in order to quantify tip force in vivo and understand the role it plays in the fungal lifestyle. The development of tuneable biocompatible materials for use in microfabricated systems offer a route to vary conditions and fully explore these variables in a species-specific manner.

6 | FUTURE PERSPECTIVES

Expansion of the use of microfabrication in fungal research in the immediately foreseeable future lies in two areas. First, although increasing numbers of labs have the equipment to generate PDMS chips from master templates, the silicon masters remain relatively expensive. Increased access to microfabrication expertise and facilities, which need not be to clean-room specification, and the availability of laser writers will establish chip technology as a mainstream laboratory method and hence broaden its application. As a result, we can expect to see imaginative new approaches to explore the diversity of fungi and their interactions, for example, with bacteria, host cells, and therapeutics (reviewed in Zhou et al., 2019). The current lack of easy access to new chip designs has lead to the one-size-fits-all approach, whereby a single design is used to test fungi of differing sizes and niche environments. Although this is of value, it means that fungal species are not examined in their own tailored environment. Second, at the pioneering end of the spectrum, the increasing complexity of chip design means that we can aim to study interconnected systems and the consequences of perturbing their many facets. Already we are moving toward systems to examine the physical and chemical interactions of fungi in complex environments using technologies such "soil-on-a-chip," plant "microbiome-on-a-chip," "human gut-on-a-chip," and "lung-on-a-chip" (Aleklett et al., 2021; Huang et al., 2021; Kim et al., 2012; Stanley & van der Heijden, 2017). Microfabrication, even in its simplest form, has already made an enormous contribution to fungal research. Its range of applications will continue to expand as chip design, new materials, imaging capability, and cross-disciplinary teamwork combine to offer ever more informed perspectives of fungal diversity and lifestyle.

CONFLICT OF INTEREST

The authors declare no conflict of interest.

DATA AVAILABILITY STATEMENT

Data sharing is not applicable to this article as no new data were created or analyzed in this study.

ORCID

Tina Bedekovic https://orcid.org/0000-0002-5315-2759
Alexandra C. Brand https://orcid.org/0000-0002-7381-131X

REFERENCES

Aleklett, K., Ohlsson, P., Bengtsson, M. & Hammer, E.C. (2021) Fungal foraging behaviour and hyphal space exploration in micro-structured Soil Chips. *ISME Journal*, *15*, 1782–1793.

Allen, E.A., Hazen, B.E., Hoch, H.C., Kwon, Y., Leinhos, G.M.E., Staples, R.C. et al. (1991) Appressorium formation in response to topographical signals by 27 rust species. *Journal of Cytology and Histology*, *81*, 323–331.

Baranger, C., Fayeulle, A. & Le Goff, A. (2020) Microfluidic monitoring of the growth of individual hyphae in confined environments. *Royal Society Open Science*, *7*, 191535.

Barker, M.G. & Walmsley, R.M. (1999) Replicative ageing in the fission yeast *Schizosaccharomyces pombe*. *Yeast*, *15*, 1511–1518.

Bedekovic, T., Agnew, E. & Brand, A.C. (2020) Rsr1 palmitoylation and GTPase activity status differentially corordinate nuclear, septin, and vacuole dynamics in *Candida albicans*. *mBio*, *11*, e01666-20.

Brand, A., Vacharaksa, A., Bendel, C., Norton, J., Haynes, P., Henry-Stanley, M. et al. (2008) An internal polarity landmark is important for externally induced hyphal behaviors in *Candida albicans*. *Eukarotic Cell*, *7*, 712–720.

Chen, K.L., Crane, M.M. & Kaeberlein, M. (2017) Microfluidic technologies for yeast replicative lifespan studies. *Mechanisms of Ageing and Development*, *161*, 262–269.

Crane, M.M., Clark, I.B.N., Bakker, E., Smith, S. & Swain, P.S. (2014) A microfluidic system for studying ageing and dynamic single-cell responses in budding yeast. *PLoS One*, *9*, e100042.

Fu, X.-H., Meng, F.-L., Hu, Y. & Zhou, J.-Q. (2008) *Candida albicans*, a distinctive fungal model for cellular aging study. *Aging Cell*, *7*, 746–757.

Fukuda, S., Yamamoto, R., Yanagisawa, N., Takaya, N., Sato, Y., Riquelme, M. et al. (2021) Trade-off between plasticity and velocity in mycelial growth. *mBio*, *12*, e03196-03120.

Gimeno, A., Stanley, C.E., Ngamenie, Z., Hsung, M.-H., Walder, F., Schmieder, S.S. et al. (2021) A versatile microfluidic platform measures hyphal interactions between *Fusarium graminearum* and *Clonostachys rosea* in real-time. *Communications Biology*, *4*, 262.

Hanson, K.L., Nicolau, D.V. Jr, Filipponi, L., Wang, L., Lee, A.P. & Nicolau, D.V. (2006) Fungi use efficient algorithms for the exploration of microfluidic networks. *Small*, *2*, 1212–1220.

Held, M., Edwards, C. & Nicolau, D.V. (2011) Probing the growth dynamics of *Neurospora crassa* with microfluidic structures. *Fungal Biology*, *115*, 493–505.

Held, M., Kašpar, O., Edwards, C. & Nicolau, D.V. (2019) Intracellular mechanisms of fungal space searching in microenvironments. *Proceedings of the National Academy of Sciences of the United States of America*, *116*, 13543–13552.

Hoch, H.C., Bojko, R.J., Comeau, G.L. & Allen, E.A. (1993) Integrating microfabrication and biology. *Circuits and Devices*, *9*, 12–22.

Huang, D., Liu, T., Liao, J., Maharjan, S., Xie, X., Pérez, M. et al. (2021) Reversed-engineered human alveolar lung-on-a-chip model. *Proceedings of the National Academy of Sciences of the United States of America*, *118*, e2016146118.

Huberts, D.H.E.W., González, J., Lee, S.S., Litsios, A., Hubmann, G., Wit, E.C. et al. (2014) Calorie restriction does not elicit a robust extension of replicative lifespan in *Saccharomyces cerevisiae*. *Proceedings of the National Academy of Sciences of the United States of America*, *111*, 11727–11731.

Jo, M.C., Liu, W., Gu, L., Dang, W. & Qin, L. (2015) High-throughput analysis of yeast replicative aging using a microfluidic system. *Proceedings of the National Academy of Sciences of the United States of America*, *112*, 9364–9369.

Kim, H.J., Huh, D., Hamilton, G. & Ingber, D.E. (2012) Human gut-on-a-chip inhabited by microbial flora that experiences intestinal peristalsis-like motions and flow. *Lab on a Chip*, *12*, 2165–2174.

Kwon, Y.H. & Hoch, H.C. (1991) Temporal and spatial dynamics of appressorium formation in *Uromyces appendiculatus*. *Experimental Mycology*, *15*, 116–131. https://doi.org/10.1016/0147-5975(91)90012-3

Last, A., Maurer, M., S Mosig, A., S Gresnigt, M. & Hube, B. (2021) In vitro infection models to study fungal–host interactions. *FEMS Microbiology Reviews*, *fuab005*, 1–22. https://doi.org/10.1093/femsre/fuab005

Lee, B., Jeong, S.-G., Jin, S.H., Mishra, R., Peter, M., Lee, C.-S. et al. (2020) Quantitative analysis of yeast MAPK signaling networks and cross-talk using a microfluidic device. *Lab on a Chip*, *20*, 2646–2655.

Lee, K.K., Labiscsak, L., Ahn, C.H. & Hong, C.I. (2016) Spiral-based microfluidic device for long-term time course imaging of *Neurospora crassa* with single nucleus resolution. *Fungal Genetics and Biology*, *94*, 11–14.

Lee, S.S., Vizcarra, I.A., Huberts, D.H.E.W., Lee, L.P. & Heinemann, M. (2012) Whole lifespan microscopic observation of budding yeast aging through a microfluidic dissection platform. *Proceedings of the National Academy of Sciences of the United States of America*, *109*, 4916–4920.

Leonhard, M., Tobudic, S., Moser, D., Zatorska, B., Bigenzahn, W. & Schneider-Stickler, B. (2013) Growth kinetics of *Candida* biofilm on medical polymers: a long-term in vitro study. *Laryngoscope*, *123*, 732–737.

Lew, R.R. (2011) How does a hypha grow? the biophysics of pressurized growth in fungi. *Nature Reviews Microbiology*, *9*, 509–518. https://doi.org/10.1038/nrmicro2591

Liu, J., Zheng, H., Poh, P.S.P., Machens, H.-G. & Schilling, A.F. (2015) Hydrogels for engineering of perfusable vascular networks. *International Journal of Molecular Sciences*, *16*, 15997–16016.

Männik, J., Teshima, R. F., Wolfrum, B. & Yang, D. (2021) Lab-on-a-chip based mechanical actuators and sensors for single-cell and organoid culture studies. *Journal of Applied Physics*, *129*(21), 210903. https://doi.org/10.1063/5.0050775

Minc, N., Boudaoud, A. & Chang, F. (2009) Mechanical forces of fission yeast growth. *Current Biology*, *19*, 1096–1101.

Money, N.P., Davis, C.M. & Ravishankar, J.P. (2004) Biomechanical evidence for convergent evolution of the invasive growth process among fungi and oomycete water molds. *Fungal Genetics and Biology*, *41*, 872–876.

Money, N.P. & Harold, F.M. (1992) Extension growth of the water mold Achlya: interplay of turgor and wall strength. *Proceedings of the National Academy of Sciences of the United States of America*, *89*, 4245–4249. https://doi.org/10.1073/pnas.89.10.4245

Nakaoka, H. & Wakamoto, Y. (2017) Aging, mortality, and the fast growth trade-off of *Schizosaccharomyces pombe*. *PLoS Biology*, *15*, e2001109.

Puerner, C., Kukhaleishvili, N., Thomson, D., Schaub, S., Noblin, X., Seminara, A. et al. (2020) Mechanical force-induced morphology changes in a human fungal pathogen. *BMC Biology*, *18*, 122. https://doi.org/10.1186/s12915-020-00833-0

Read, N.D., Kellock, L.J., Collins, T.J. & Gundlach, A.M. (1997) Role of topography sensing for infection-structure differentiation in cereal rust fungi. *Planta*, *202*, 163–170.

Riquelme, M., Gierz, G. & Bartnicki-Garcia, S. (2000) Dynein and dynactin deficiencies affect the formation and function of the Spitzenkörper and distort hyphal morphogenesis of *Neurospora crassa*. *Microbiology*, *146*, 1743–1752.

Riquelme, M., Reynaga-Pena, C.G., Gierz, G. & Bartnicki-Garcia, S. (1998) What determines growth direction in fungal hyphae? *Fungal Genetics and Biology*, *24*, 101–109. https://doi.org/10.1006/fgbi.1998.1074

Ryley, J. & Pereira-Smith, O.M. (2006) Microfluidics device for single cell gene expression analysis in *Saccharomyces cerevisiae*. *Yeast*, *23*, 1065–1073.

Saka, Y., MacPherson, M. & Giuraniuc, C.V. (2017) Generation and precise control of dynamic biochemical gradients for cellular assays. *Physica A: Statistical Mechanics and its Applications*, *470*, 132–145. https://doi.org/10.1016/j.physa.2016.11.134

Stanley, C.E. & Van der Heijden, M.G.A. (2017) Microbiome-on-a-Chip: new frontiers in plant–microbiota research. *Trends in Microbiology*, *25*, 610–613.

Sun, Y., Tayagui, A., Garrill, A. & Nock, V. (2018) Fabrication of in-channel high-aspect ratio sensing pillars for protrusive force measurements on fungi and oomycetes. *Journal of Microelectromechanical Systems*, *27*, 827–835.

Sun, Y., Wan, K.-T., Roberts, K.P., Bischof, J.C. & Nelson, B.J. (2003) Mechanical property characterization of mouse zona pellucida. *IEEE Transactions on NanoBioscience*, *2*, 279–286.

Thomson, D.D., Wehmeier, S., Byfield, F.J., Janmey, P.A., Caballero-Lima, D., Crossley, A. et al. (2015) Contact-induced apical asymmetry drives the thigmotropic responses of *Candida albicans* hyphae. *Cellular Microbiology*, *17*, 342–354.

Uehling, J.K., Entler, M.R., Meredith, H.R., Millet, L.J., Timm, C.M., Aufrecht, J.A. et al. (2019) Microfluidics and metabolomics reveal symbiotic bacterial–fungal interactions between *Mortierella elongata* and *Burkholderia* Include metabolite exchange. *Frontiers in Microbiology*, *10*, 2163.

Wang, P., Robert, L., Pelletier, J., Dang, W.L., Taddei, F., Wright, A. et al. (2010) Robust growth of *Escherichia coli*. *Current Biology*, *20*, 1099–1103.

Witkowski, D., Kubicki, W., Dziuban, J.A., Jašíková, D. & Karczemska, A. (2018) Micro-particle image velocimetry for imaging flows in passive microfluidic mixers. *Metrology and Measurement Systems*, *25*, 441–450.

Zhou, W., Le, J., Chen, Y., Cai, Y., Hong, Z. & Chai, Y. (2019) Recent advances in microfluidic devices for bacteria and fungus. *Trends in Analytical Chemistry*, *112*, 175–195.

How to cite this article: Bedekovic, T. & Brand, A.C. (2021) Microfabrication and its use in investigating fungal biology. *Molecular Microbiology*, 00, 1–9. https://doi.org/10.1111/mmi.14816